ELSEVIER

Thin Solid Films 299 (1997) 178–182

thin solid films

Dependence of the *C*49–*C*54 $TiSi_2$ phase transition temperature on film thickness and Si substrate orientation

Hyeongtag Jeon [a], Gangjoong Yoon [a], R.J. Nemanich [b]

[a] *Department of Metallurgical Engineering, Hanyang University, Seoul 133-791, South Korea*
[b] *Department of Physics, North Carolina State University, Raleigh, NC 27695, USA*

Received 22 February 1996; accepted 13 June 1996

Abstract

The *C*49 to *C*54 phase transition and the surface and interface morphologies were examined for titanium silicides formed on atomically clean Si substrates. The properties were explored as a function of the Ti film thickness, deposition temperature and Si substrate orientation. Ti films of thicknesses between 5 nm and 40 nm were deposited at elevated temperatures from 500 °C to 900 °C in increments of 100 °C onto Si(100) and Si(111) wafers. The titanium silicides are analyzed with X-ray diffraction, Raman, scanning and transmission electron microscopy for phase identification and measurement of the surface and interface morphologies. The *C*49 to *C*54 $TiSi_2$ phase transition is observed to occur between 600 °C and 700 °C for the thickest films on (100) wafers, but the transition temperature is observed to increase as the film thickness is decreased or for films formed on Si(111) substrates. For a 20 nm Ti film deposited onto Si(100), the transition temperature occurs between 600 °C and 700 °C. However, for the same thickness of Ti on Si(111), the transition temperature is found between 700 °C and 800 °C. This retardation of the phase transition is discussed in terms of surface and volume free-energy considerations.

Keywords: Phase transition; Titanium silicide; Silicon

1. Introduction

With the continuing increase in the densities of Si semiconductor devices, new gate and interconnection materials with low resistivity and high temperature stability are required [1]. Refractory metal silicides such as $TiSi_2$, WSi_2, $TaSi_2$ and $MoSi_2$ have been studied extensively because of their low resistivity and high temperature stability. $TiSi_2$ among these materials shows the lowest resistivity (12.4 $\mu\Omega$ cm) [2], high temperature stability, and compatibility with current processing. As such, $TiSi_2$ is considered to be good material for application in ultra large scale integration (ULSI) [3–5]. Two significant problems limit the application of titanium silicides into Si devices: the *C*49–*C*54 phase transition temperature and the agglomeration of the silicide during the annealing processes [6–8].

The $TiSi_2$ formed by thin film reaction has two different structures: the *C*49 structure (base-centered orthorhombic) which is formed between 450 °C and 650 °C, and the *C*54 structure (face-centered orthorhombic) which is formed above 650 °C. The *C*49 $TiSi_2$ is known to be a metastable phase and is usually observed to be the first crystal phase to form in the thin film reaction of Ti and Si [9,10]. The *C*54 $TiSi_2$ phase is the stable phase which has a lower resistivity than the *C*49 phase. Both crystal structures exhibit similar atom arrangements in the atomic planes with a hexagonal array of Si atoms around Ti atoms at the center, but the unit cell of each phase shows a different stacking arrangement (e.g. the *C*49 phase has a two-layer repeat while the *C*54 phase has a four-layer repeat).

In this study, we focus our attention on the phase retardation of the titanium silicide. Ti thin films were deposited onto atomically clean Si(100) and Si(111) wafers. The phase identification of each titanium silicide was accomplished with Raman scattering and X-ray diffraction (XRD). The surface and interface morphologies of the *C*49 and *C*54 $TiSi_2$ phases were analyzed by scanning and transmission electron microscopy (SEM and TEM). The results of the phase identification show that the phase transition temperature is increased (or retarded) depending on the Ti film thickness and the Si substrate orientation [4,11,12]. The results are discussed in terms of the surface and volume free energies.

2. Experimental details

The substrates used in this study were Si(111) and Si(100) oriented wafers (25 mm diameter) with resistivity

0040-6090/97/$17.00 © 1997 Elsevier Science S.A. All rights reserved
PII S0040-6090(96)09042-6

of 0.8–1.2 Ω cm (n-type, P doped). The ultrahigh vacuum (UHV) system was equipped with a turbopumped loading chamber and an ion-pumped UHV chamber with two stations for deposition and analysis. The deposition station has a heating stage and Ti filament deposition source, and the analysis stage has low-energy electron diffraction (LEED) and Auger electron spectroscopy (AES) characterization. The base pressure in the UHV chamber was less than 1×10^{-10} Torr. Before loading, the wafers were cleaned by a UV–ozone exposure [13,14] and a spin etch with $HF+H_2O+$ethanol (1:1:10) at room temperature [15]. The wafer was then loaded into the UHV system and heated to a temperature of 800 °C for 10 min to desorb the residual contaminants and hydrogen [16]. The chamber pressure was typically less than approximately 1×10^{-9} Torr during the heat cleaning. After heat cleaning, the base pressure returned to $(1–2)\times10^{-11}$ Torr. Following the in situ cleaning, the LEED showed either 2×1 Si(100) or 7×7 Si(111) diffraction patterns and AES indicated no evidence of oxygen or carbon [17]. The Ti films were then deposited at elevated temperatures from 500 °C to 900 °C onto the Si(100) and (111) substrates, and the film thicknesses were monitored with a quartz crystal monitor. The Ti deposition rates were about 0.2 nm s^{-1}. The phase identification of the grown layers of $TiSi_2$ was carried out with XRD and Raman scattering. Surface and interface morphologies of the films were observed with SEM and TEM.

3. Results

The Ti films of 5 nm to 40 nm thickness were deposited onto Si(100) and Si(111) in UHV, and titanium silicides were formed by annealing at temperatures between 500 °C and 900 °C. The phase transition temperature was determined by XRD and Raman. Table 1 is a summary of the observed crystal phases of the $TiSi_2$ films on Si(100) in the temperature range 500–900 °C. For the Ti films of 40 nm and 20 nm thickness, the *C*49 to *C*54 transition temperature occurs between 600 °C and 700 °C. However, for silicides formed from Ti films less than 10 nm thick, an increased transition temperature was observed. For Ti films of 10 nm on Si(100), the phase transition occurs between 700 °C and 800 °C while for Ti films of 5 nm, the *C*49 phase is stable up to 800 °C. Table 2 presents a summary of the observed crystal structures of the $TiSi_2$ films on Si(111) in the temperature range 500–900 °C. For Ti films of 40 nm on Si(111), the transition to the *C*54 phase occurs at a temperature between 600 °C and 700 °C, while for Ti films of 20 nm, the transition occurs at a temperature between 700 °C and 800 °C which is about 100 °C higher than the transition temperature observed for similar films on Si(100). For the Ti films under 10 nm thick, the *C*49 phase is stable up to 800 °C. These results show that the phase transition temperature is increased as the Ti film thickness is reduced, and this retardation is more significant on Si(111) than on Si(100).

Table 1
Summary of titanium silicide phases on Si(100) identified by XRD and Raman scattering

Thickness (nm)	Temperature (°C)				
	500	600	700	800	900
5	*C*49	*C*49	*C*49	*C*49	Not detected
10	*C*49	*C*49	*C*49	*C*54	*C*54
20	*C*49	*C*49	*C*54	*C*54	*C*54
40	*C*49	*C*49	*C*54	*C*54	*C*54

Table 2
Summary of titanium silicide phases on Si(111) identified by XRD and Raman scattering

Thickness (nm)	Temperature (°C)				
	500	600	700	800	900
5	Not detected	*C*49	*C*49	*C*49	Not detected
10	Not detected	*C*49	*C*49	*C*49	Not detected
20	*C*49	*C*49	*C*49	*C*54	*C*54
40	*C*49	*C*49	*C*54	*C*54	*C*54

Fig. 1 displays the surface morphologies of $TiSi_2$ on Si(100) and Si(111) surfaces formed at temperatures of 500 °C, 700 °C and 900 °C. Fig. 2 shows the interface morphologies of each sample as observed by TEM. These results display the surface morphologies of both the *C*49 and *C*54 phases on both Si(100) and Si(111) surfaces. The surface morphology of the *C*49 phase exhibits significant pit formation while that of the *C*54 phase shows $TiSi_2$ islands at various stages of coalescence. The interface morphologies of the *C*49 and *C*54 phase show wavy and relatively smooth characters respectively.

4. Discussion

In this study the $TiSi_2$ films were formed by thin film reactions in UHV (thus eliminating effects due to contamination). The important result of this experiment is that the *C*49 to *C*54 phase transition temperature depends on the Ti film thickness and Si substrate orientation. The increased temperature for thinner films indicates that the phase transition is retarded. Generally the metastable *C*49-$TiSi_2$ phase is formed at low temperatures (450–650 °C) and the stable *C*54-$TiSi_2$ phase at high temperatures (above 650 °C), but in this experiment the phase transition temperature depended on both the Ti film thickness and the Si substrate orientation. In order to discuss this retardation of the phase transition of $TiSi_2$, we consider the variation in the free energy vs. film thickness. Previously we have shown that islanding and the initial *C*49 phase nucleation could be ascribed to similar effects based on the surface and interface energies [11]. To discuss the temperature dependence of the phase transformation, we assume that the initial titanium silicide was

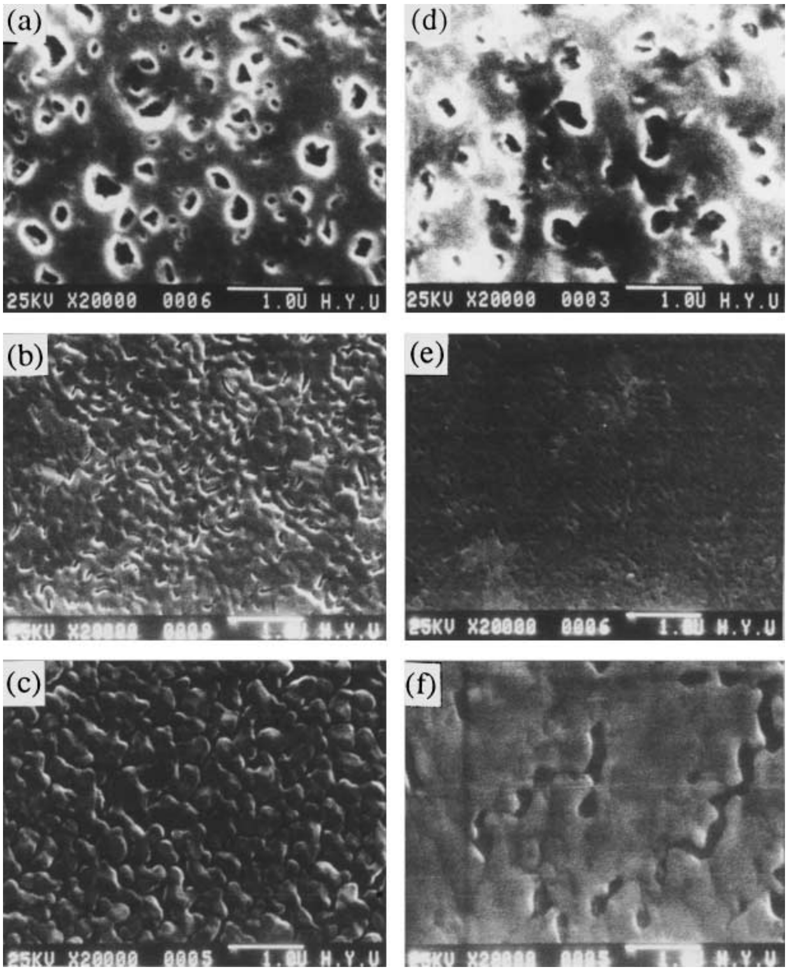

Fig. 1. SEM images of titanium silicide formed from 40 nm of Ti deposited onto Si(100) at (a) 500 °C, (b) 700 °C, (c) 900 °C and onto Si(111) at (d) 500 °C, (e) 700 °C, (f) 900 °C.

formed uniformly (i.e. the energies of the boundaries between silicide grains are not significant). We define the Si substrate surface energy, the $TiSi_2$/Si interface energy and the $TiSi_2$ surface energy as γ_1, γ_2, and γ_3 respectively. For the bulk energies it is necessary to obtain the ratio of atoms consumed from the film and substrate. To form a titanium silicide of thickness *t*, 0.4*t* of the Ti film and 0.9*t* of the Si substrate are consumed. Therefore the free energy change ΔG to form titanium silicide is

$$\Delta G = A[(G_{0\mathrm{TiSi2}} - 0.4G_{0\mathrm{Ti}} - 0.9G_{0\mathrm{Si}})t + \gamma_3 + \gamma_2 - \gamma_1] \quad (1)$$

The free energy change per unit area is then given by

$$\begin{aligned}\Delta G/A &= [(G_{0\mathrm{TiSi2}} - 0.4G_{0\mathrm{Ti}} - 0.9G_{0\mathrm{Si}})t + \gamma_3 + \gamma_2 - \gamma_1] \\ &= \Delta G_0 t = \Delta\gamma \qquad (2)\end{aligned}$$

where ΔG_0 is the volume term and $\Delta\gamma$ is the surface/interface term of the Gibbs free energy change. This equation describes the free energy change per unit area as a function of the titanium silicide film thickness *t*. A schematic representation of this equation is shown in Fig. 3. The intercept at the vertical axis defines the surface/interface free energy change $\Delta\gamma$ and the slope of the line is the volume free energy difference ΔG_0. The surface/interface free energy term $\Delta\gamma$ here includes both the surface energy and the interface energy between $TiSi_2$ and Si.

If we apply Eq. (2) to the *C*49 and *C*54 phases of $TiSi_2$, we can explain the retardation of the phase transition. Since the *C*54 phase is the stable phase of $TiSi_2$, the values of ΔG_0 are given by $G_{0C54} < G_{0C49} < 0$. Similarly, since the *C*49 phase is the first phase to nucleate, but has the higher volume free energy, we can conclude that $\Delta\gamma_{C49} < \Delta\gamma_{C54}$ [11]. The curves are different for the different substrate orientations since for Si, the surface and interface free energies of the (111) surface are lower than those of the (100) surface. The driving force for the *C*49 to *C*54 phase transition at any thickness *t,* is the energy difference of the two free energy lines. As is evident in Fig. 3, the driving force for the phase transition decreases as the film thickness is decreased. Similarly, the driving force for the phase transition of the silicide film on Si(100) becomes greater than that on Si(111). The results of this experiment can then be explained by these considerations based on the volume and surface and interface energies. The transition temperature is known to be about 650 °C for films with thickness greater than 40 nm. However, for

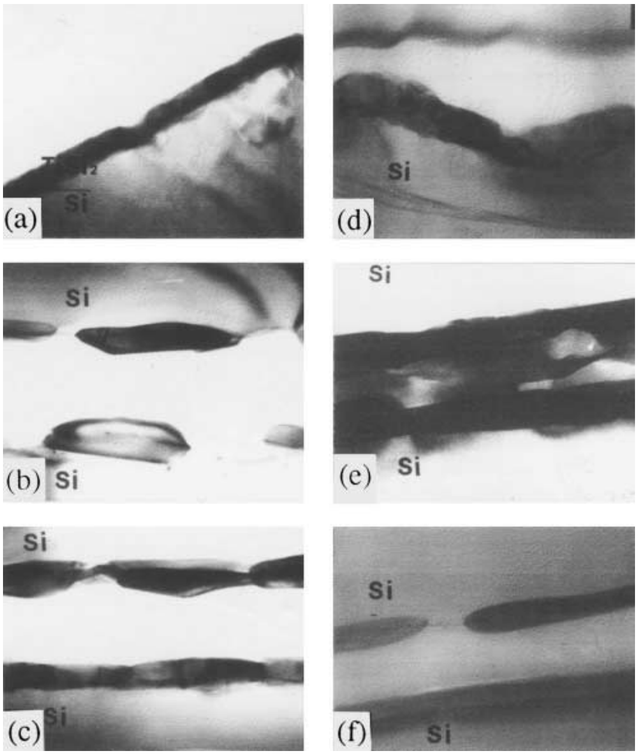

Fig. 2. TEM cross-section images of titanium silicide formed from 40 nm of Ti deposited onto Si(100) at (a) 500 °C, (b) 700 °C, (c) 900 °C and onto Si(111) at (d) 500 °C, (e) 700 °C, (f) 900 °C.

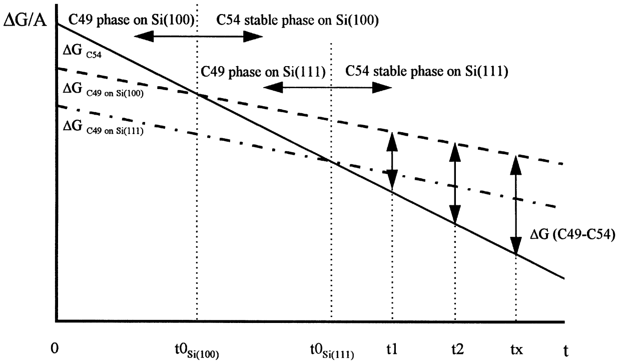

Fig. 3. Schematic relationship of the free energy per unit area vs. film thickness of the *C*49 and *C*54 $TiSi_2$ on Si(100) and Si(111).

the thin Ti films less than 20 nm, the phase transition temperature begins to increase up to 800 °C with decreasing Ti film thickness. This increase in transition temperature can be ascribed to kinetic considerations. Since the driving force decreases as the film thickness is decreased, therefore the transition temperature must be increased to nucleate the *C*54 phase. This is indicated schematically in Fig. 3, where at t_2 we represent the energetics for 40 nm of Ti and at t_1 we represent the energetics for 10 nm of Ti. Then the driving force ΔG_1 at t_1 is much smaller than the driving force ΔG_2 at t_2.

According to Fig. 3 the driving force is decreased as the film thickness is decreased, and ultimately there exists a (critical) film thickness at which the driving force $\Delta G_{C49-C54}$ is zero. For thicknesses less than this critical thickness the *C*49 metastable phase becomes stable. Therefore, independent of annealing temperature and time, the phase transition from *C*49 to *C*54 will not occur below this critical thickness. From the experimental results presented here, the critical thickness is about 12.5 nm (titanium silicide thickness) on Si(100) and 25 nm (titanium silicide thickness) on Si(111). The experimental results of others show similar results indicating that the phase transition for 13 nm titanium silicide grown by chemical vapor deposition does not occur up to 850 °C [2].

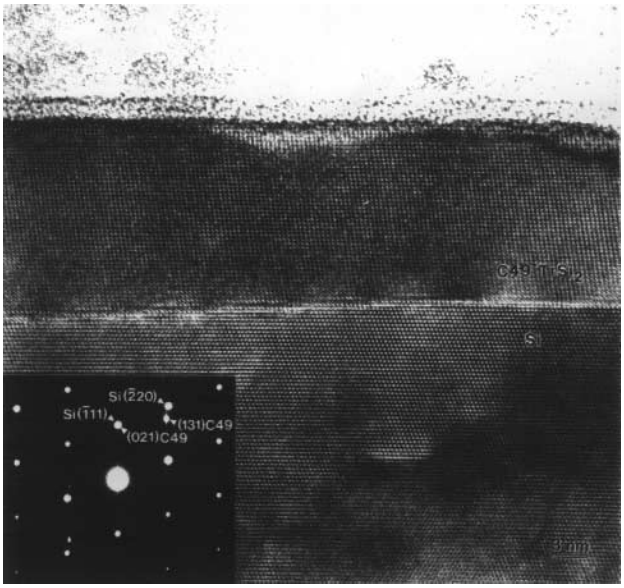

Fig. 4. HRTEM cross-section image of *C*49 $TiSi_2$ on Si(111).

The results also show that the Si substrate orientation affects the phase transition temperature. As shown in Table 1 and Table 2, the titanium silicide on Si(111) shows a significant increase in the transition temperature compared with the temperature for a similar silicide thickness on Si(100). This dependence on substrate orientation is attributed to the lower surface and interface energies of Si(111) compared with those of Si(100) [11]. The lower interface energy of the Si(111) may be a result of the silicide interface structure. As shown in Fig. 4, the interface of $TiSi_2$/Si(111) exhibits a pseudomorphic character. It is likely that the epitaxial registry of the *C*49 $TiSi_2$ on Si(111) has a much lower interface energy than the heteroepitaxial $TiSi_2$ on Si(100). According to Fig. 3, the driving force for the phase transition is decreased significantly owing to the lower interface energy of $TiSi_2$/Si(111).

5. Summary

In this study, we have investigated the retardation of the *C*49 to *C*54 phase transition of $TiSi_2$. Two effects were observed. As the Ti film thickness is decreased below 40 nm, the *C*49–*C*54 $TiSi_2$ transition temperature increases, and the transition temperature is further increased for (111) oriented Si substrates vs. Si(100). The volume and surface/interface free energies were considered, and the driving force of the transition was modeled. The transition temperature effects were related from kinetic considerations based on the magnitude of the driving force of the transition. According to these considerations, the *C*49–*C*54 transition temperature depends on the Ti film thickness and also on the orientation of the Si substrate. The orientation effect is attributed to different surface and interface energies. TEM results indicate a pseudomorphic character of the *C*49 $TiSi_2/Si(111)$ interface which should result in a low interface energy. The model also predicts that the *C*49 phase is the stable phase for film thicknesses less than a critical thickness. The experimentally determined critical thickness is found to be about 12.5 nm of $TiSi_2$.

Acknowledgements

This study was supported by the Korea Science and Engineering Foundation through grant KOSEF 931-0800-012-2 and 951-0801-016-2.

References

[1] S.P. Murarka, *Silicides for VLSI Applications*, Academic Press, New York, 1983.

[2] J. Engqvist, U. Jansson, J. Lu and J. Carlsson, *J. Vac. Sci. Technol. A, 12* (1994) 161.

[3] S.P. Murarka and D.B. Fraser, J. Appl. Phys., 51 (1980) 342.

[4] F.M. d'Heurle, *J. Mater. Res., 3* (1988) 167.

[5] M.D. Nacem, W.A. Orr-Arienzo and J.G. Rapp, *Appl. Phys. Lett., 66* (1995) 877.

[6] P. Revesz, L.R. Zheng, L.S. Hung and J.W. Mayer, *Appl. Phys. Lett., 48* (1986) 1591.

[7] S. Ogawa, T. Yoshida and T. Kouzaki, *Appl. Phys. Lett., 56* (1990) 725.

[8] T. Yoshida, S. Ogawa, S. Okuda, T. Kouzaki and K. Tsukamoto, *J. Electrochem. Soc., 137* (1990) 1914.

[9] R. Beyers and R. Sinclair, *J. Appl. Phys., 57* (1985) 5240.

[10] M.H. Wang and L.J. Chen, *Appl. Phys. Lett., 59* (1991) 2460.

[11] H. Jeon, C.A. Sukow, T.W. Honeycutt, G.A. Rozgonyi and R.J. Nemanich, *J. Appl. Phys., 71* (1992) 4269.

[12] J.W. Mayer and S.S. Lau, *Electronic Materials Science*, Macmillan, New York, 1990.

[13] J.R. Vig, *J. Vac. Sci. Technol. A, 3* (1985) 1023.

[14] K.L. Mittal (ed.), *Treatise on Clean Surface Technology*, Vol. 1, Plenum, New York, 1987.

[15] D.B. Fenner, D.K. Biegelsen and R.D. Bringans, *J. Appl. Phys., 66* (1988) 419.

[16] A. Ishizaka and Y. Shiraki, *J. Electrochem. Soc., 133* (1986) 666.

[17] A. Cantana, P.E. Schmid, M. Heintze and F. Levy, *J. Appl. Phys., 67* (1990) 1820.